C: Surfaces, Interfaces, Porous Materials, and Catalysis

Elucidating the Structure of the Cu-Alkaline Electrochemical Interface with the Laser-Induced Jump Temperature Method

Paula Sebastian-Pascual, Francisco J. Sarabia, Victor Climent, Juan Miguel Feliu, and María Escudero-Escribano

J. Phys. Chem. C, **Just Accepted Manuscript** • DOI: 10.1021/acs.jpcc.0c07821 • Publication Date (Web): 23 Sep 2020

Elucidating the structure of the Cu-alkaline electrochemical interface with the laser-induced jump temperature method

Paula Sebastián-Pascual[1], Francisco J. Sarabia[2], Víctor Climent[2], Juan M. Feliu[2], María Escudero-Escribano[1]**

[1]Department of Chemistry, University of Copenhagen, Universitetsparken 5, 2100 Copenhagen, Denmark

[2]Instituto Universitario de Electroquímica, University of Alicante, C./ San Vicente del Raspeig s/n, 03690 San Vicente del Raspeig, Spain

*Corresponding author:

E-mail: maria.escudero@chem.ku.dk

E-mail: victor.climent@ua.es

Abstract

Detailed description of the Cu-electrolyte interface is vital to understand the electrocatalytic properties of Cu surfaces. Herein, we combine cyclic voltammetry and the laser induced temperature jump technique to describe the structure of Cu(111) and Cu(100) | electrolyte interfaces in 0.1 M NaOH in a glass-free electrochemical cell. Laser-induced potential transients recorded at different potentials provided information of the surface charge distribution, which allowed us to calculate the potential of maximum entropy (*pme*), which can be considered a good estimation of the potential of zero charge (*pzc*) of Cu(111) and Cu(100). We found that $pzc_{Cu(111)} > pzc_{Cu(100)}$, following the same order as their respective work functions values. Interestingly, the estimated *pzc* appears located at the onset potential of the OH* voltammetric feature for Cu(111) and Cu(100), which suggests that this feature shifts with the *pzc* of each crystallographic orientation. This is the first study that provides experimental evidence of the charge distribution at the Cu-solution interface under alkaline conditions.

Table of contents graphic

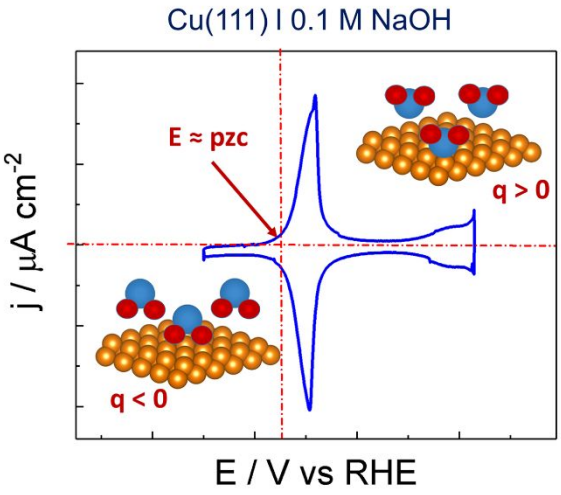

Cu is the only pure metal that can reduce CO_2 beyond CO to produce hydrocarbon fuels and valuable chemicals.[1–6] Due to its singular electrocatalytic properties for sustainable CO_2 conversion, fundamental studies with the purpose to provide detailed description of the interfacial properties of Cu electrocatalysts are receiving an increasing attention.[7–13] In particular, studies on well-defined Cu single-crystalline electrodes are key to build the bridge between theoretical calculations, usually conducted on model surfaces,[2,3] and experiments.[9,14,15]

Single-crystalline electrodes are terminated in a well-oriented surface. Because of that, single crystal electrodes have been traditionally used to explore and find the relations between surface structure and catalytic properties in electrochemical energy conversion reactions,[16–19] such as the CO_2 reduction reaction.[20,21] Furthermore, they allow to elucidate electrolyte effects on the electrocatalytic properties, including the effect of pH and both cations and anions interacting with the surface and reaction intermediates.[11,12,22–25] Despite the importance of using Cu single-crystalline electrodes in electrocatalysis, their interfacial and surface structure properties have been scarcely investigated, especially in alkaline media, a desirable electrolyte for the CO reduction on Cu.[3,9,14,26]. In particular, the number of studies combining electrochemical characterization with other in-situ techniques, such as spectroscopy techniques[10,12,25,27,28] or scanning tunneling microscopy (STM), for surface structure characterization,[29–32] is even more limited.

Importantly, blank cyclic voltammograms (CVs) of Cu single-crystalline electrodes in alkaline media are being currently reviewed.[8,9,13] Blank CVs of single-crystalline surfaces constitute a fingerprint that can be used as an *in situ* control parameter of the cleanliness conditions and quality of the surfaces employed. Recently, it has been demonstrated that blank CVs of Cu(hkl) in alkaline media are highly sensitive to the presence of dissolved glass.[8] Tiwari et al. observed that the multiple splitting of peaks[33] on the Cu(111) | 0.1 M NaOH CVs is caused by the presence in

solution of metal traces from the corrosion of the glass under alkaline conditions. This was demonstrated by using cyclic voltammetry and inductively coupled plasma mass spectrometry (ICP) for chemical analysis of metallic traces in the electrolyte. Notably, experiments carried out in the absence of glass have shown that only a quasi-reversible pair of peaks appear centered at 0.1 V vs RHE, attributed to the presence of specifically adsorbed OH on <111> terraces.[8–10,13,29,30] In their report, surface ordering of employed surfaces was also confirmed by STM. This type of works highlight the need to report clean and reproducible CVs of Cu single-crystalline surfaces for a rigorous assessment of their electrocatalytic properties.[34]

Description of the Cu-electrolyte interface requires the determination of the values of the real potential of zero charge (*pzc*), i.e., the potential value at which the capacitive excess (free) charge on the surface is zero.[35] This is an intrinsic property of the metal-electrolyte interface highly relevant for rational description of the electrified double layer structure and also water solvent structure[35,36]. Importantly, the *pzc* is related with the work function of the metal electrode (ϕ) (*i.e.*, the minimum energy required to remove one electron at the fermi level of the specific metallic phase), modified by the contact with the electrolyte.[37] Reporting experimental data that estimates the values of *pzc* of the different Cu facets is crucial to describe electrostatic interactions at the double layer region. It has been recently reported that the electrocatalytic activity of some reactions can be tuned by simply altering the charge distribution on the surface through the deposition of small coverages of adsorbates that shift the *pzc* of the surface. This is the case of $Ni(OH)_x$ deposited on Pt, which showed enhanced performance for the hydrogen evolution reaction (HER) compared to pristine Pt due to, among other effects, a restructuration of the solvent network induced by a potential shift of the *pzc*.[16,38,39] Thus, reporting data on the interfacial properties on Cu single-

crystalline electrodes is of paramount importance for rational tuning of its electrocatalytic properties.

Despite the importance of reporting the *pzc of Cu*, there are only very few reports addressing this question.[40,41] Bellier and Lecoeur [41] performed capacitive measurements in neutral solutions and claimed that the difference between the *pzc* of Cu(111) and Cu(100) in neutral media is around 0.34 V, in agreement with work function expectations, since work function decreases with the atomic density of the surface. In this case, $\phi_{Cu(100)} < \phi_{Cu(111)}$. Hori and co-workers conducted voltammetric CO displacement measurements on different Cu(S)[n(111)x(100)] stepped surfaces and in phosphate solutions. They suggested that the characteristic CO voltammetric peak shifts linearly with the corresponding work functions, providing relative measurement of *pzc* values of Cu surfaces in aqueous solution.[40,42] It is important to remark that the CO displacement technique provides information of the total charge distribution on the surface, which means that it does not differentiate between free excess charge and faradic charge originated by electrolyte specific adsorption (e.g. hydrogen or hydroxide adsorption/desorption processes).[42]

In recent years, the laser-induced temperature jump technique has emerged as a potential tool for experimental determination of the *pzc* of a wide range of single-crystalline surfaces. Those surfaces include non-polarizable surfaces such as Pt or Ir[16,38,43–45] in which the capacitive or free excess charge appears coupled with the specific hydrogen or hydroxide adsorption/desorption. The laser technique allows to decouple the capacitive charge processes from faradic contribution for indirect estimation of the *pzc*.[43,44] This technique applies short pulses of laser to an electrode surface to suddenly increase the interfacial temperature. The sudden increase of the temperature (T) of the metal-electrolyte interface results in a shift of the electrode potential. This change on the electrode potential (E_M) is monitored at constant charge (q), in the microsecond time scale, giving

a measure of the thermal coefficient of the potential drop: $\left(\frac{\partial E_M}{\partial T}\right)_q$. The change of the electrode potential has been demonstrated to be mainly related with the change on the dipolar contribution of the solvent to the interfacial potential drop, while specific adsorption is decoupled due to its lower rate.[43] Since solvent dipoles orientate with the electric field on the surface, the magnitude and sign of the recorded potential-time transient is indicative of the free charge distribution on the surface. The applied potential value at which the laser-induced potential transient is zero can be identified with the potential of maximum entropy (*pme*) of double layer formation. It has been demonstrated for other model surfaces, such as Pt(111)[46] and Au(111)[47] that the potential of maximum entropy is located close to the *pzc*, because the main driving force for the dipolar orientation is the electric field at the interphase, which is dominated by the free charge separation between metal and solution phases.

Here we combine cyclic voltammetry and laser-induced temperature jump measurements to investigate the Cu(100) and Cu(111) | 0.1 M NaOH interfaces. Special attention has been taken to avoid contamination from the attack of glass by the alkaline solution. We have conducted laser-induced potential transients at different applied potentials inside the pseudocapacitive region of both Cu(100) and Cu(111), to determine, for the first time, the *pzc* of each surface. This study provides key insights on the interfacial properties of Cu(100) and Cu(111) that would be helpful for a deeper understanding of electrocatalytic reactions of interest, such as the CO_2 and the CO reduction on Cu. Details of the experiments and employed techniques are provided in the supporting information (S.I.).

We start assessing the surface ordering of the employed Cu single crystalline electrodes and cleanliness of the system by reproducing blank CVs from the literature.[8,9] Fig. 1 shows the blank CVs of both Cu(100) (Fig. 1A) and Cu(111) (Fig. 1B) in contact with a 0.1 M NaOH solution.

CVs were recorded in a perfluoroalcoxy alkane (PFA) electrochemical cell, to avoid traces of contamination from the attack of dissolved glass by the alkaline solution in a convectional glass cell (Fig. S1 from the supporting information). Cu single-crystal surfaces were pre-treated by electropolishing, as described in the S.I. Obtained blank CVs of Cu(100) and Cu(111) essentially display the same main features that in previous reports,[7–9] thus validating the employed procedures that we use to pretreat the electrode surface. Cu(100) presents a quasi-reversible pair of peaks centered at -0.15 V vs RHE, related with adsorbed OH.[9] We also see the characteristic pair of irreversible peaks on Cu(100) around 0.47 V vs RHE, which are indicative of high-surface ordering degree and are likely related with the first stages of surface oxidation.[7] Cu(111) blank CV (Fig. 2B) only displays a couple of quasi-symmetric pair of peaks at 0.10 V vs RHE, also related with adsorbed OH on <111> terraces.[9] Here, we have also carried out blank CVs in a conventional glass cell to confirm that the presence of traces of glass components in solution causes the multi-splitting of the main OH-peak, as demonstrated by Tiwari et al. [8] (Fig. S2). Interestingly, while Cu(111) CVs are highly affected by the employed electrochemical cell material (PFA or glass), Cu(100) blank CV remains unchanged. Despite the lack of sensitivity of Cu(100) to the contamination from the glass, the CV on Cu(111) clearly shows the presence of undesirable contaminant traces in solution, which must be avoided since they could affect the electrocatalytic properties of Cu.[34]

Figure 1C shows the blank CV of Cu(111) at different selected potential windows. Fig 1C a) and b) displays short window blank CVs, showing that the voltammetric profile remains stable in the potential range between -0.45 V and 0.40 V vs RHE. However, the decrease of the lower potential limit, close to the hydrogen evolution reaction (HER), affects dramatically the voltammetric profile of Cu(111). First, the peak at 0.1 V vs RHE in the anodic direction, becomes broader and

shifts to more positive potential values. Second, the counter-peak in the cathodic direction decreases in intensity and loses charge (Fig. 1C,d and Fig S3A). This shows that solvent reduction involving the HER affect the surface properties and could induce some surface passivation.[28,48] Cycling in the short potential window between -0.40 V and 0.3 V vs RHE, causes the appearance of the main features in the blank CV, which disappeared because of solvent reduction (Fig S3B). Our recent voltammetric study shows that the Cu(111) evolves surfaces passivation in both phosphate and bicarbonate solutions, and the passivation phenomenon does not depend on the bulk pH solution.[13] The recorded blank CV of Cu(111) in 0.1 M NaOH solution confirms that passivation of <111> does not depend on the electrolyte. This phenomenon deserves consideration, for instance, to stablish the potential conditions in the CO reduction in alkaline media. It is worth to remark that Cu(100) also evolves surface changes under reductive conditions and induced by the HER, despite that the voltammetric profiles in the pseudocapacitive region remains stable.[7,11] Surface-reordering under HER conditions on Cu(100) has been thoroughly demonstrated by using scanning tunneling microscopy.[31,49,50] In the following sections, we report results of the laser induced-potential transients avoiding the low potential region, aiming to detect the *pzc* of pristine Cu(111) and Cu(100).

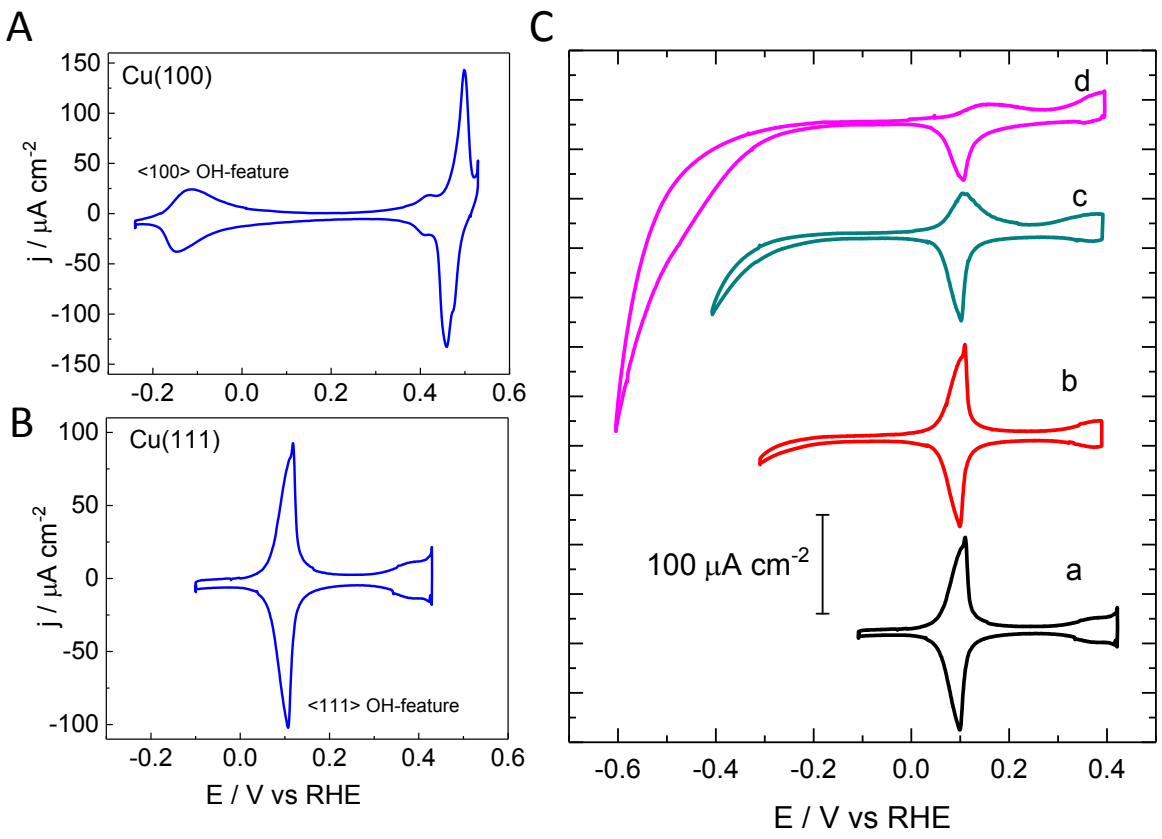

Figure 1: Blank cyclic voltammograms of Cu single-crystalline electrodes in contact with 0.1 M NaOH solution. A) Cu(100), B) Cu(111) and C) Cu(111) under different potential limits. Scan rate: 50 mV/s.

After checking the quality and surface ordering of both Cu(111) and Cu(100) electrodes in alkaline conditions, we test also the single-crystalline electrodes in the electrochemical cell for in-situ laser-induced temperature jump experiments. As described in the supporting information, the electrolyte is confined in a small space between a Teflon cone, positioned over a quartz window, through which the laser beam reaches the surface (Fig. S4). Blank CVs essentially show the same voltammetric features already reported (Fig. S5). In particular, the Cu(111) blank CVs only present the pair of non-split peaks centered at 0.1V vs RHE, that remains unaltered after the laser

experiment, thus demonstrating the stability of the quartz window and the absence of glass components in the solution (Fig. S5C).

Fig. 2 shows the laser-induced potential transients for both Cu(100) (Fig. 2A) and Cu(111) (Fig. 2B) electrodes, at different applied potentials within the pseudocapacitive potential window between 0.4 V and -0.4 V vs RHE. We observe, on both Cu(100) and Cu(111), that the laser-potential transients are positive at sufficiently high applied potentials (between 0.07 V and 0.32 V vs RHE on Cu(111), and between -0.15 V and 0.40 V vs RHE on Cu(100)), thus indicating that the free charge on the surface remains positive. Decreasing the applied potential causes a decrease in intensity of the potential transient, until the sign of the transient changes to a negative value at low enough potentials. This indicates that at those potential values, the free charge on the surface is negative, and the negative polarization increases by continuing decreasing the applied potential.

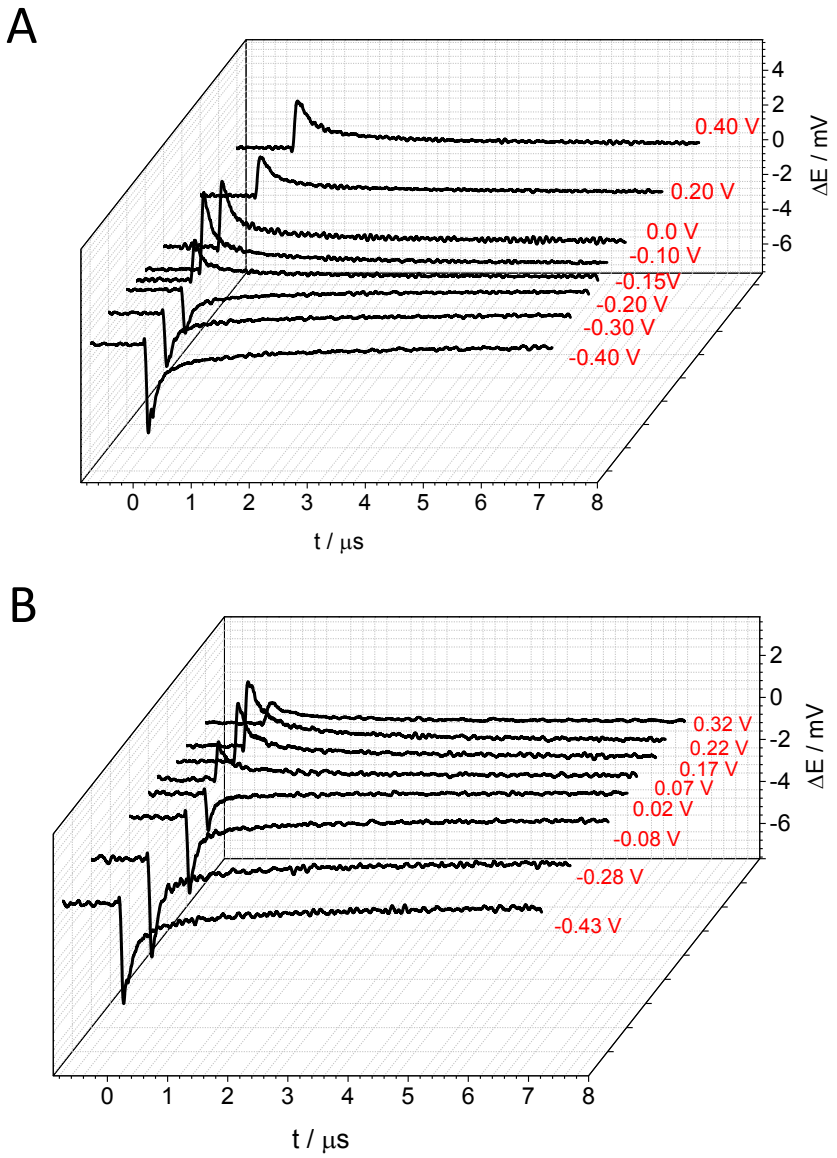

Figure 2: Laser induced-potential transients at different applied potentials for: A) Cu(100) | 0.1 M NaOH and B) Cu(111) | 0.1 M NaOH.

Interestingly, Fig. 2 shows that all recorded potential-transient in between these two potential limits (0.4 V and -0.4 V vs RHE) show a monotonous decay. Non-monotonous or bipolar responses have been observed on Pt electrodes associated to adsorption reactions or slow responses

of the solvent.[43,45] A bipolar or non-monotonous laser transient would signal the overlapping of different processes with different rates in the microsecond time scale, such as double layer restructuration and ion specific adsorption. The absence of such non-monotonous response suggest that the main contribution to the change of the electrode potential is due to solvent restructuration. Other processes, such as specific anion adsorption, appear decoupled in the microsecond time scale because either they do not take place or they are too slow to contribute to the potential change.[45]

Because the solvent restructuration is fast enough in the microsecond time-scale it can be concluded that the change of the electrode potential follows the relaxation of the temperature. A simple heat transfer model shows that temperature relaxation follows a $t^{-1/2}$decay (see S.I.), that allows linearization of the potential transients (Fig. S6). The slope of the linearized potential-transients at any applied potential value is proportional to the thermal coefficient of the interfacial potential drop, *i.e.*, to the electrode potential change with temperature ($\partial E_M/\ \partial T$ in mVK^{-1}). These coefficients are positive if the charge on the surface is positive, or negative for a negatively charged surface.[47] In Fig. 3, we have plotted the thermal coefficients ($\partial E_M/\ \partial T$) at different applied potential conditions for Cu(100) (Fig. 3A, top panel) and Cu(111) (Fig. 3A, bottom panel). In both electrodes, the applied potential at which ($\partial E_M/\ \partial T$) has zero value, is the potential of maximum entropy (*pme*) which is closely related to the *pzc*. Calculated values of the *pme* were: 0.060±0.019 V vs RHE for Cu(111), and -0.170 ±0.005 V vs RHE for Cu(100). Fig. 3A clearly shows that the *pme* of Cu(111) is higher than the *pme* of Cu(100).

We have compared the difference between the $pme_{Cu(111)}$ and $pme_{Cu(100)}$ obtained in this work with the difference between their corresponding work functions (ϕ/e) in Fig 3B). We observe that the difference between *pme* values, which is around 230 mV, approaches the difference between their

reported work function values, which ranches between 170 and 300 mV, and follows the order $\phi_{Cu(100)} < \phi_{Cu(111)}$.[51–53] Our results show good agreement with the work function expectations, and that the small discrepancy between calculated *pme* and work function values is possibly due to two main reasons: i) the inherent high error associated to the calculation of work function values on metallic surfaces (Figure 3B).[54] ii) The interactions between electrode surface and the electrolyte (0.1 M NaOH) possibly influences the interfacial properties of Cu surfaces thus affecting the estimation of the corresponding *pme* value of Cu single-crystalline electrodes.[44]

Interestingly, the *pme* of both Cu(111) and Cu(100) is located at the onset potential of the OH voltammetric feature (Fig. 1A and B). On both Cu(111) and Cu(100), negative transients appear at potentials below the OH adsorption feature, suggesting that OH appears adsorbed on a positively charged surface. This result highlights that this structure feature most likely shifts with the corresponding *pzc* of Cu single-crystalline electrodes, *i.e.*, it seems to be strongly affected by the charge distribution on the surface. In a recent report by Sarabia et al.,[55] the *pme* of Pt basal planes in alkaline media has been measured. The *pme* of Pt(111) also appears located at the onset of the OH adsorption feature. In addition, the OH adsorption features on the other basal planes (Pt(110) and Pt(100)) also shift with their respective *pme* values, towards lower potential values, in agreement with their respective work function values. This behavior is in agreement with our observation on the *pme* and the OH feature on both Cu(111) and Cu(100). Another plausible explanation to the coincidence of the *pme* with the onset of OH adsorption would be that the incipient OH layer on Cu could induce the turning of the water molecules to a preferential orientation with the oxygen toward the electrode surface, due to a chemical hydrogen bond interaction between the OH and water molecules. Such chemical preference for the oxygen down configuration would slightly shift the *pme* towards lower potentials in comparison with the *pzc*. In

spite of that, the good correlation between the *pme* of both Cu(111) and Cu(100) with their work function differences supports that the specific free charge distribution on each single crystalline surface dominates on the potential-induced laser response and, therefore the *pme* is a good estimation of the *pzc* of Cu electrodes. Our work clearly shows that the properties of the Cu(hkl)-electrolyte interface are affected by the electronics of each orientation which are modified by solvent-electrolyte interactions, in agreement with earlier studies on other metal-electrolyte interfaces.[43–45,55] Future work in progress will aim to elucidate the effect of using different electrolytes (e.g. solutions containing bicarbonate or phosphate anions) and pH on the potential-induced laser response as well as on the interfacial properties of Cu single crystalline electrodes.

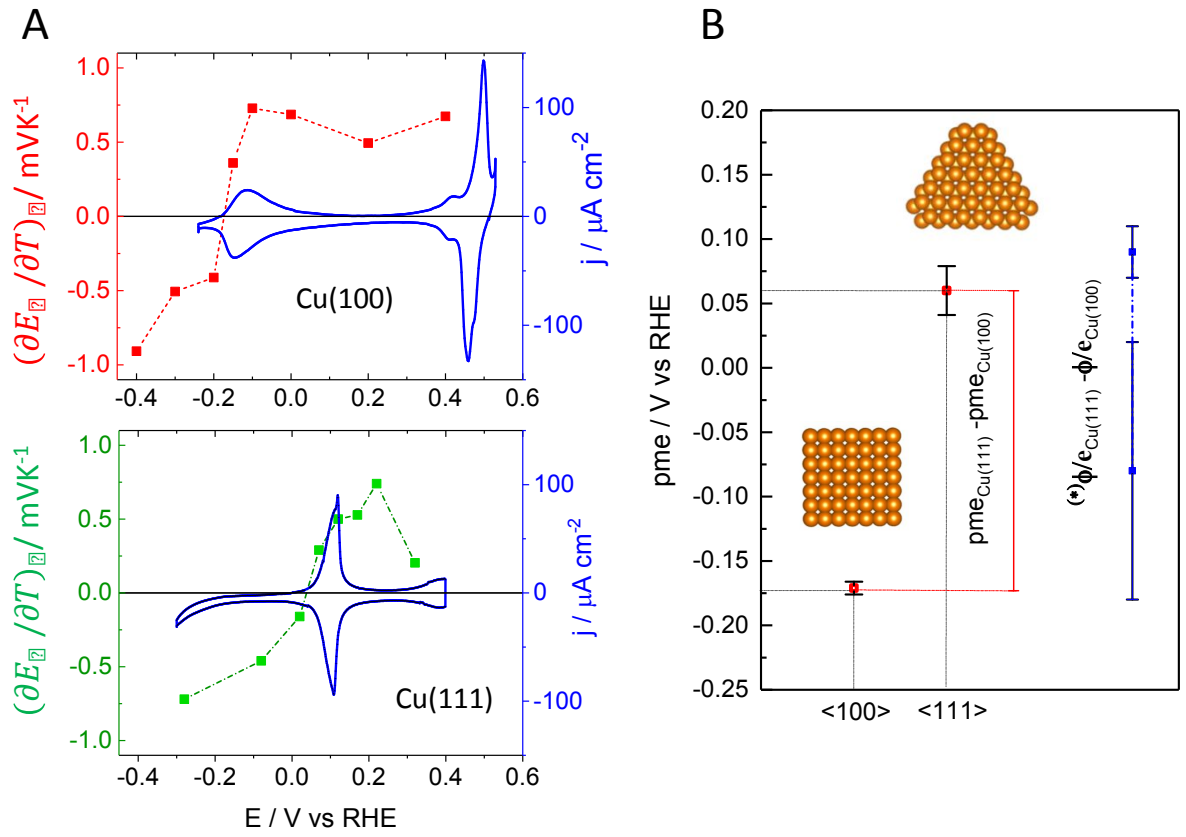

Figure 3: A) Representation of the thermal coefficients (dE_M/dT) at different applied potential and with the corresponding blank cyclic voltmmetries of: Top panel) Cu(100) | 0.1 M NaOH. Bottom panel) Cu(111) | 0.1 M NaOH. B) Potential of maximum entropy values of both Cu(100) and Cu(111) in 0.1 M NaOH solution, plotted against the difference between the work function values. (*) Data obtained from ref [41,53,54]. We also show the errors associated to the measurement of the work function values and the *pme* of Cu surfaces.

In summary, we report, for the first time, an estimation of the values of *pzc* of clean Cu(111) and Cu(100) in contact with a 0.1 M NaOH solution through the calculation of the potential of maximum entropy (*pme)* by use of the laser-induced jump temperature methodology. We observe

that the *pme* of Cu(111) is higher than the *pme* of Cu(100), in agreement with the work function values of the corresponding single-crystalline electrodes. Remarkably, we observe that the *pme* appears closely located at potentials lower to the main feature of the blank CVs, related to specifically adsorbed OH. The laser experiment suggests that this OH-feature shifts with the corresponding *pzc* value of Cu single crystals. Herein we want to highlight the importance of reporting clean cyclic voltammograms of Cu single-crystalline electrodes, not only while assessing both their surface and interfacial properties, but also for further reliable analysis of the CO and CO_2 reduction. We have also demonstrated that the laser-induced temperature jump method is a valuable experimental tool providing relevant information in relation to water structure, interfacial properties of Cu electrodes and surface charge distribution. We believe that this technique could be employed for further rationalization of the CO_2 reduction reaction, especially while assessing electric field, solvent and pH effects on this complex reaction.

SUPPORTING INFORMATION

Additional experiments carried out on Cu(111) and Cu(100) electrodes in the laser-jump temperature cell are included in the supporting information. Detailed description of experimental details and full analysis of potential-induced laser transients is also included.

AUTHOR INFORMATION

Corresponding author:

*E-mail: maria.escudero@chem.ku.dk

*E-mail: victor.climent@ua.es

ORCID

Paula Sebastián-Pascual: 0000-0001-7985-0750

Víctor Climent: 0000-0002-2033-5284.

Juan Miguel Feliu Martínez: 0000-0003-4751-3279

María Escudero-Escribano: 0000-0002-6432-3015

Notes

The authors declare no competing financial interest.

ACKNOWLEDGMENT

M.E.-E. gratefully acknowledges the Villum Foundation for the award of a Villum Young Investigator Grant (project number: 19142). J.M.F. thanks the MCINN (FEDER) (Spain) project-PID2019-105653GB-100.

REFERENCES

(1) Nitopi, S. A.; Bertheussen, E.; Scott, S. B.; Liu, X.; Albert, K.; Horch, S.; Seger, B.; Stephens, I. E. L.; Chan, K.; Nørskov, J. K.; et al. Progress and Perspectives of Electrochemical CO_2 Reduction on Copper in Aqueous Electrolyte. *Chem. Rev.* **2018**, *119* (12), 7610–7672.

(2) Bagger, A.; Ju, W.; Varela, A. S.; Strasser, P.; Rossmeisl, J. Electrochemical CO_2 Reduction: Classifying Cu Facets. *ACS Catal.* **2019**, *9* (9), 7894–7899.

(3) Bagger, A.; Arnarson, L.; Hansen, M. H.; Spohr, E.; Rossmeisl, J. Electrochemical CO Reduction: A Property of the Electrochemical Interface. *J. Am. Chem. Soc.* **2019**, *141* (4), 1506–1514.

(4) Hori, Y.; Murata, A.; Takahashi, R.; Suzuki, S. Electroreduction of CO to CH_4 and C_2H_4 at a Copper Electrode in Aqueous Solutions at Ambient Temperature and Pressure. *J. Am. Chem. Soc.* **1987**, *109* (16), 5022–5023.

(5) Hori, Y.; Takahashi, I.; Koga, O.; Hoshi, N. Selective Formation of C2 Compounds from Electrochemical Reduction of CO_2 at a Series of Copper Single Crystal Electrodes. *J. Phys. Chem. B* **2002**, *106* (1), 15–17.

(6) Bagger, A.; Ju, W.; Varela, A. S.; Strasser, P.; Rossmeisl, J. Electrochemical CO_2 Reduction: A Classification Problem. *ChemPhysChem* **2017**, *18* (22), 3266–3273.

(7) Chorkendorff, I.; Horch, S.; Engstfeld, A. K.; Stephens, I. E. L.; Maagaard, T. Polycrystalline and Single-Crystal Cu Electrodes: Influence of Experimental Conditions on the Electrochemical Properties in Alkaline Media. *Chem. - A Eur. J.* **2018**.

(8) Tiwari, A.; Maagaard, T.; Chorkendorff, I.; Horch, S. Effect of Dissolved Glassware on

the Structure-Sensitive Part of the Cu(111) Voltammogram in KOH. *ACS Energy Lett.* **2019**, *4* (7), 1645–1649.

(9) Tiwari, A.; Heenen, H. H.; Bjørnlund, A. S.; Maagaard, T.; Cho, E.; Chorkendorff, I.; Kristoffersen, H. H.; Chan, K.; Horch, S. Fingerprint Voltammograms of Copper Single Crystals under Alkaline Conditions: A Fundamental Mechanistic Analysis. *J. Phys. Chem. Lett.* **2020**, *11* (4), 1450–1455.

(10) Bodappa, N.; Su, M.; Zhao, Y.; Le, J.-B.; Yang, W.-M.; Radjenovic, P.; Dong, J.-C.; Cheng, J.; Tian, Z.-Q.; Li, J.-F. Early Stages of Electrochemical Oxidation of Cu(111) and Polycrystalline Cu Surfaces Revealed by in Situ Raman Spectroscopy. *J. Am. Chem. Soc.* **2019**, *141* (31), 12192–12196.

(11) Pérez-Gallent, E.; Marcandalli, G.; Figueiredo, M. C.; Calle-Vallejo, F.; Koper, M. T. M. Structure- and Potential-Dependent Cation Effects on CO Reduction at Copper Single-Crystal Electrodes. *J. Am. Chem. Soc.* **2017**, *139* (45), 16412–16419.

(12) Pérez-Gallent, E.; Figueiredo, M. C.; Calle-Vallejo, F.; Koper, M. T. M. Spectroscopic Observation of a Hydrogenated CO Dimer Intermediate During CO Reduction on Cu(100) Electrodes. *Angew. Chemie - Int. Ed.* **2017**, *56* (13), 3621–3624.

(13) Sebastián-Pascual, P.; Escudero-Escribano, M. Addressing the Interfacial Properties for CO Electroreduction on Cu with Cyclic Voltammetry. *ACS Energy Lett.* **2020**, *5* (1), 130–135.

(14) Bagger, A.; Arán-Ais, R. M.; Halldin Stenlid, J.; dos Santos, E.; Arnarson, L.; Degn Jensen, K.; Escudero-Escribano, M.; Roldan Cuanya, B.; Rossmeisl, J. Ab Initio Cyclic Voltammetry on Cu(111), Cu(100) and Cu(110) in Acidic, Neutral and Alkaline

Solutions. *ChemPhysChem* **2019**, *20*, 1–11.

(15) Varela, A. S.; Schlaup, C.; Jovanov, Z. P.; Malacrida, P.; Horch, S.; Stephens, I. E. L.; Chorkendorff, I. CO2 Electroreduction on Well-Defined Bimetallic Surfaces: Cu Overlayers on Pt(111) and Pt(211). *J. Phys. Chem. C* **2013**, *117* (40), 20500–20508.

(16) Ledezma-Yanez, I.; Wallace, W. D. Z.; Sebastián-Pascual, P.; Climent, V.; Feliu, J. M.; Koper, M. T. M. Interfacial Water Reorganization as a PH-Dependent Descriptor of the Hydrogen Evolution Rate on Platinum Electrodes. *Nat. Energy* **2017**, *2*, 17031.

(17) Jensen, K. D.; Tymoczko, J.; Rossmeisl, J.; Bandarenka, A. S.; Chorkendorff, I.; Escudero-Escribano, M.; Stephens, I. E. L. Elucidation of the Oxygen Reduction Volcano in Alkaline Media Using a Copper–Platinum(111) Alloy. *Angew. Chemie - Int. Ed.* **2018**, *57* (11), 2800–2805.

(18) Dong, J.-C.; Zhang, X.-G.; Briega-Martos, V.; Jin, X.; Yang, J.; Chen, S.; Yang, Z.-L.; Wu, D.-Y.; Feliu, J. M.; Williams, C. T.; et al. In Situ Raman Spectroscopic Evidence for Oxygen Reduction Reaction Intermediates at Platinum Single-Crystal Surfaces. *Nat. Energy* **2019**, *4* (1), 60–67.

(19) Arán-Ais, R. M.; Scholten, F.; Kunze, S.; Rizo, R.; Roldan Cuenya, B. The Role of in Situ Generated Morphological Motifs and Cu(i) Species in C2+ Product Selectivity during CO_2 Pulsed Electroreduction. *Nat. Energy* **2020**, 5, 317-325.

(20) Birdja, Y. Y.; Pérez-Gallent, E.; Figueiredo, M. C.; Göttle, A. J.; Calle-Vallejo, F.; Koper, M. T. M. Advances and Challenges in Understanding the Electrocatalytic Conversion of Carbon Dioxide to Fuels. *Nat. Energy* **2019**, *4* (9), 732–745.

(21) Sebastián-Pascual, P.; Mezzavilla, S.; Stephens, I. E. L.; Escudero-Escribano, M. Structure-Sensitivity and Electrolyte Effects in CO_2 Electroreduction: From Model Studies to Applications. *ChemCatChem* **2019**, *11* (16), 3626–3645.

(22) Schouten, K. J. P.; Pérez Gallent, E.; Koper, M. T. M. Structure Sensitivity of the Electrochemical Reduction of Carbon Monoxide on Copper Single Crystals. *ACS Catal.* **2013**, *3* (6), 1292–1295.

(23) Hori, Y.; Koga, O.; Watanabe, Y.; Matsuo, T. FTIR Measurements of Charge Displacement Adsorption of CO on Poly- and Single Crystal (100) of Cu Electrodes. *Electrochim. Acta* **1998**, *44* (8–9), 1389–1395.

(24) Reske, R.; Mistry, H.; Behafarid, F.; Roldan Cuenya, B.; Strasser, P. Particle Size Effects in the Catalytic Electroreduction of CO_2 on Cu Nanoparticles. *J. Am. Chem. Soc.* **2014**, *136* (19), 6978–6986.

(25) Koga, O.; Watanabe, Y.; Tanizaki, M.; Hori, Y. Specific Adsorption of Anions on a Copper (100) Single Crystal Electrode Studied by Charge Displacement by CO Adsorption and Infrared Spectroscopy. *Electrochim. Acta* **2001**, *46* (20–21), 3083–3090.

(26) Figueiredo, M. C.; Trieu, V.; Eiden, S.; Koper, M. T. M. Spectro-Electrochemical Examination of the Formation of Dimethyl Carbonate from CO and Methanol at Different Electrode Materials. *J. Am. Chem. Soc.* **2017**, *139* (41), 14693–14698.

(27) Niaura, G. Surface-Enhanced Raman Spectroscopic Observation of Two Kinds of Adsorbed OH− Ions at Copper Electrode. *Electrochim. Acta* **2000**, *45* (21), 3507–3519.

(28) Heyes, J.; Dunwell, M.; Xu, B. CO_2 Reduction on Cu at Low Overpotentials with Surface-

Enhanced in Situ Spectroscopy. *J. Phys. Chem. C* **2016**, *120* (31), 17334–17341.

(29) Kunze, J.; Maurice, V.; Klein, L. H.; Strehblow, H.-H.; Marcus, P. In Situ Scanning Tunneling Microscopy Study of the Anodic Oxidation of Cu(111) in 0.1 M NaOH. *J. Phys. Chem. B* **2001**, *105* (19), 4263–4269.

(30) Kunze, J.; Maurice, V.; Klein, L. H.; Strehblow, H.-H.; Marcus, P. In Situ STM Study of the Anodic Oxidation of Cu(001) in 0.1 M NaOH. *J. Electroanal. Chem.* **2003**, *554–555*, 113–125.

(31) Kim, Y.-G.; Javier, A.; Baricuatro, J. H.; Torelli, D.; Cummins, K. D.; Tsang, C. F.; Hemminger, J. C.; Soriaga, M. P. Surface Reconstruction of Pure-Cu Single-Crystal Electrodes under CO-Reduction Potentials in Alkaline Solutions: A Study by Seriatim ECSTM-DEMS. *J. Electroanal. Chem.* **2016**, *780*, 290–295.

(32) Maurice, V.; Strehblow, H.-H.; Marcus, P. In Situ STM Study of the Initial Stages of Oxidation of Cu(111) in Aqueous Solution. *Surf. Sci.* **2000**, *458* (1), 185–194.

(33) Klaas, K. J.; Gallent, E. P.; Koper, M. T. M. The Electrochemical Characterization of Copper Single-Crystal Electrodes in Alkaline Media. *J. Electroanal. Chem.* **2013**, *699*, 6–9.

(34) Hori, Y.; Konishi, H.; Futamura, T.; Murata, A.; Koga, O.; Sakurai, H.; Oguma, K. “deactivation of Copper Electrode” in Electrochemical Reduction of CO_2. *Electrochim. Acta* **2005**, *50* (27), 5354–5369.

(35) Climent, V.; Feliu, J. M. Thirty Years of Platinum Single Crystal Electrochemistry. *J. Solid State Electrochem.* **2011**, *15* (7–8), 1297–1315.

(36) Trasatti S., L. E. The Potential of Zero Charge. *White R.E., Bockris J.O., Conw. B.E. Mod. Asp. Electrochem. Mod. Asp. Electrochem. Springer, Boston, MA* **2002**, *33*.

(37) García-Aráez, N.; Climent, V.; Feliu, J. M. Evidence of Water Reorientation on Model Electrocatalytic Surfaces from Nanosecond-Laser-Pulsed Experiments. *J. Am. Chem. Soc.* **2008**, *130* (12), 3824–3833.

(38) Sarabia, F. J.; Sebastián-Pascual, P.; Koper, M. T. M.; Climent, V.; Feliu, J. M. Effect of the Interfacial Water Structure on the Hydrogen Evolution Reaction on Pt(111) Modified with Different Nickel Hydroxide Coverages in Alkaline Media. *ACS Appl. Mater. Interfaces* **2019**, *11* (1), 613–623.

(39) Morales-Guio, C. G.; Cave, E. R.; Nitopi, S. A.; Feaster, J. T.; Wang, L.; Kuhl, K. P.; Jackson, A.; Johnson, N. C.; Abram, D. N.; Hatsukade, T.; et al. Improved CO_2 Reduction Activity towards C2+ Alcohols on a Tandem Gold on Copper Electrocatalyst. *Nat. Catal.* **2018**, *1* (10), 764–771.

(40) Koga, O.; Matsuo, T.; Hoshi, N.; Hori, Y. Charge Displacement Adsorption of Carbon Monoxide on [110] Zone Copper Single Crystal Electrodes in Relation with PZC. *Electrochim. Acta* **1998**, *44* (6–7), 903–907.

(41) Bellier, J. L. J. P. De Charge Nulle D ' Electrodes De Cuivre D ' Orientation Et (100) Au Contact De Solutions De Potassium. *Electrochim. Acta* **1985**, *30* (1), 1027–1033.

(42) Martínez-Hincapié, R.; Sebastián-Pascual, P.; Climent, V.; Feliu, J. M. Exploring the Interfacial Neutral PH Region of Pt(111) Electrodes. *Electrochem. commun.* **2015**, *58*, 62–64.

(43) Garcia-Araez, N.; Climent, V.; Feliu, J. Potential-Dependent Water Orientation on Pt(111), Pt(100), and Pt(110), As Inferred from Laser-Pulsed Experiments. Electrostatic and Chemical Effects. *J. Phys. Chem. C* **2009**, *113* (21), 9290–9304.

(44) Ganassin, A.; Sebastián, P.; Climent, V.; Schuhmann, W.; Bandarenka, A. S.; Feliu, J. On the PH Dependence of the Potential of Maximum Entropy of Ir(111) Electrodes. *Sci. Rep.* **2017**, *7* (1), 1246.

(45) Sebastián, P.; Martínez-Hincapié, R.; Climent, V.; Feliu, J. M. Study of the Pt (111) | Electrolyte Interface in the Region Close to Neutral PH Solutions by the Laser Induced Temperature Jump Technique. *Electrochim. Acta* **2017**, *228*, 667–676.

(46) Climent, V.; Coles, B. A.; Compton, R. G. Coulostatic Potential Transients Induced by Laser Heating of a Pt(111) Single-Crystal Electrode in Aqueous Acid Solutions. Rate of Hydrogen Adsorption and Potential of Maximum Entropy. *J. Phys. Chem. B* **2002**, *106* (23), 5988–5996.

(47) Climent, V.; Coles, B. A.; Compton, R. G. Laser-Induced Potential Transients on a Au(111) Single-Crystal Electrode. Determination of the Potential of Maximum Entropy of Double-Layer Formation. *J. Phys. Chem. B* **2002**, *106* (20), 5258–5265.

(48) Schlaup, C.; Horch, S. In-Situ STM Study of Phosphate Adsorption on Cu(111), Au(111) and Cu/Au(111) Electrodes. *Surf. Sci.* **2013**, *608*, 44–54.

(49) Matsushima, H.; Taranovskyy, A.; Haak, C.; Gründer, Y.; Magnussen, O. M. Reconstruction of Cu(100) Electrode Surfaces during Hydrogen Evolution. *J. Am. Chem. Soc.* **2009**, *131* (30), 10362–10363.

(50) Kim, Y. G.; Baricuatro, J. H.; Javier, A.; Gregoire, J. M.; Soriaga, M. P. The Evolution of the Polycrystalline Copper Surface, First to Cu(111) and Then to Cu(100), at a Fixed CO_2RR Potential: A Study by Operando EC-STM. *Langmuir* **2014**, *30* (50), 15053–15056.

(51) Lide, D. R.; Frederikse, H. P. R. CRC Handbook of Chemistry and Physics; 1998.

(52) Hölzl, J.; Schulte, F. K. Work Functions of Metals. In *In Solid Surface Physics*; Höhler, G., Ed.; 1979.

(53) P. O. Gartland, S. Berge, and B. J. S. Photoelectric Work Function of a Copper Single Crystal for the (100), (110), (111), and (112) Faces. *Phys Chem Rev lett.* **1972**, *28* (738).

(54) Derry, G. N.; Kern, M. E.; Worth, E. H. Recommended Values of Clean Metal Surface Work Functions. *J. Vac. Sci. Technol. A* **2015**, *33* (6), 60801.

(55) Sarabia, F. J.; Sebastián, P.; Climent, V.; Feliu, J. M. New Insights into the Pt(hkl)-Alkaline Solution Interphases from the Laser Induced Temperature Jump Method. *J. Electroanal. Chem.* **2020**, 114068, DOI:10.1016/j.jelechem.2020.114068.